Quantification of clarithromycin polymorphs in presence of tablet excipients.

Swathi Kuncham[a], Ganesh Shete[a] and Arvind Kumar Bansal[*]

[a]Department of Pharmaceutics, National Institute of Pharmaceutical Education and Research (NIPER), S.A.S. Nagar, Punjab 160 062, India

Received: January 20, 2014; *Accepted:* March 2, 2014

Original Article

ABSTRACT

Excipients can cause a considerable challenge when developing a solid form of an active pharmaceutical ingredient (API). The aim of this present study was to analyze the polymorphs of clarithromycin (CAM) mixed with excipients using powder X-ray diffraction (PXRD). Polymorphic Form I (CAM-1), Form II (CAM-2) and an amorphous phase of CAM were characterized using thermal and crystallographic methods. CAM-1 and CAM-2 were monotropically related, with CAM-2 being the stable form. PXRD instrument related parameters were optimized for the characterization of CAM polymorphic forms using a variety of excipients. Calibration curves for CAM-1 and CAM-2 mixed with excipients were also prepared. Analytical methods based on the differences in the diffraction patterns of CAM-1, CAM-2 and the excipients were developed. Sodium methyl paraben, sodium propyl paraben, microcrystalline cellulose and magnesium stearate were crystalline showing characteristic diffraction patterns. Starch, croscarmellose sodium, talc and sodium starch glycolate were semicrystalline in nature, while colloidal silicon dioxide was amorphous. A diffraction peak at 8.7° 2θ provided a quantification of CAM-2 when mixed with excipients. The analytical method was evaluated and validated for accuracy, precision, inter- and intra-day variation, variability due to sample repacking and instrument reproducibility. The method for quantification of CAM-2 in the range of 80 to 100% w/w was linear with $R^2 = 0.998$. Relative standard deviation (RSD), due to sample repacking, was 2.77% indicating good homogeneity of mixing of the samples. RSD due to assay errors was 1.66%. PXRD analysis of the commercial tablet showed the CAM-2 as a major polymorph being 98% of the overall content of the API. CAM-1 was found to be present as an impurity at trace levels shown by peaks at 2θ values of 5.2° and 6.7°. This method provides a method for characterization of the polymorphic forms of CAM in the presence of commonly used excipients. It could be a useful tool for monitoring solid form behavior during product development and stability studies.

KEY WORDS: Clarithromycin, powder X-ray diffraction, polymorph quantification, solid state characterization, tablet excipients

INTRODUCTION

The oral route is used extensively for the administration of (APIs) and the most commonly used form is solid dosage such as tablets and capsules. The solid state properties of an API can have a profound influence on the performance of the dosage form (1). Polymorphism is an important solid state property which should be considered during the development of the formulation (2).

* Corresponding author: Department of Pharmaceutics, National Institute of Pharmaceutical Education and Research (NIPER), S.A.S. Nagar, Punjab 160 062, India, E-mail: akbansal@niper.ac.in, bansalarvind@yahoo.com, Tel: +91-172- 2214682 Ext. 2126, Fax: +91-172- 2214692

Polymorphic forms of the same API can have different physical and chemical properties including melting point, chemical reactivity, apparent solubility, dissolution rate, optical and mechanical properties (compaction behavior, flow properties), vapor pressure and density (3). The presence of polymorphs in various proportions in the formulation can affect the stability, dissolution and bioavailability of the API (4). There are also stringent regulatory requirements for the identification and quantification of the polymorphs (5).

The ICH Q6A guideline provides a decision tree for the determination of polymorphism of the API indicating whether a change in polymorphism could have an effect on the final product performance (6). The guideline proposes a decision for "investigating the need to set acceptance criteria for polymorphism in drug substance and drug products". Should the final drug product be affected by polymorphic forms it may require monitoring of the polymorph during stability testing (paragraph 3 of the decision tree) (6). Therefore it may be necessary to quantify the polymorphic contents of the API in the solid dosage form (7).

A variety of techniques, such as, powder X-ray diffractometry (PXRD), spectroscopy (Raman, mid- and near-IR), solid state NMR and thermal techniques have been used for the quantification of polymorphic forms in polymorphic mixtures (8). PXRD is used extensively because it is simple and, non-destructive in nature. Some of the APIs that have previously been evaluated for their polymorphic contents in binary mixtures containing two polymorphs by PXRD include carbamazepine, clopidogrel bisulphate and olanzapine (9-11).

The characterization and quantification of an API polymorphic form in the presence of excipients poses challenges due to the (i) dilution of the API concentration, and (ii) peak shift and interference in the diffraction pattern of the API caused by diffraction patterns of the excipients (12-14). Most previous studies analyzed the polymorphic content of the API in a polymorphic mixture (9-11). However, less attention has been paid to the quantification of polymorphs in finished dosage forms that are mixed with excipients.

The present study was based on using PXRD to characterize the polymorphs of clarithromycin (CAM) and quantify its polymorphs (Form I and II) in a solid dosage form mixed with excipients. CAM is a macrolide antibiotic used in the treatment of otitis media, pharyngitis, tonsillitis, sinusitis, duodenal ulcer disease and Lyme's disease. It exists in several polymorphic forms, e.g., Form-0 (ethanolate), Form-I (metastable polymorph), Form-II (stable polymorph), Form-III (acetonitrile solvate), Form-IV (monohydrate) and Form-V (15-17). Form-II is the most stable polymorph at ambient conditions and is used in commercial tablet formulations. The chemical structure of CAM is shown in Figure 1.

MATERIALS AND METHODS

Materials

CAM polymorphic Form-I (CAM-1) and Form-II (CAM-2) were received as gifts from Ind-Swift Lab. Ltd., Solan, India.

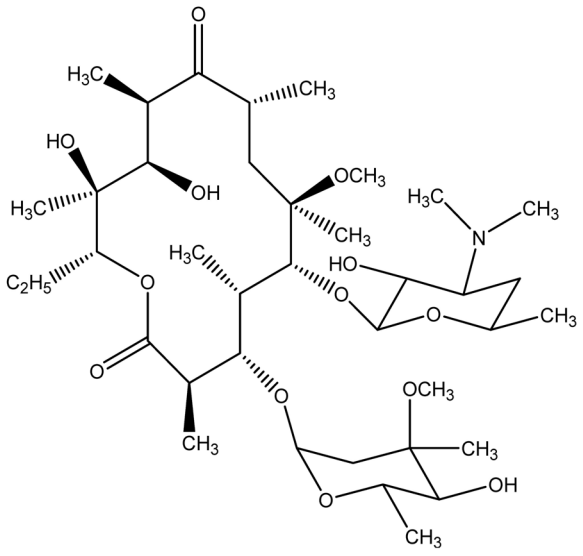

Figure 1 Chemical structure of CAM

The samples were >99% pure as stated on the certificate of analysis provided by the manufacturer. Starch NF was purchased from Lobachemie Pvt. Ltd., Mumbai, India. Avicel® (microcrystalline cellulose NF) was supplied by the FMC group, Brussels, Belgium. Sodium methyl paraben NF and sodium propyl paraben NF were gifts from Ranbaxy Lab. Ltd., Gurgaon, India. Croscarmellose sodium NF was supplied by Signet Chemical Corp. Pvt. Ltd., Mumbai, India. Magnesium stearate NF was supplied by Fine Chemical Lab., Bangalore, India. Aerosil 200® (colloidal silicon dioxide NF) was supplied by Evonik Industries, Hanau, Germany. Sodium starch glycolate NF was supplied by Penwest Pharmaceuticals Co., New York, USA (now JRS Pharma LP). Talc NF was purchased from Lobachemie Pvt. Ltd., Mumbai, India. All the materials were used as received.

Methods

Solid state characterization

Microscopy

Powder samples were analyzed using a Leica DMLP polarizing microscope (Leica Microsystems, GmbH, Wetzlar, Germany) under bright and cross-polarized light equipped with Linkam LTS 350 Hot stage at 200X magnification. Photomicrographs were obtained using a JVC color video camera and analyzed using Linksys32 software (v. 1.8.9). The distribution of the particle size, taken as the length along the longest axis of the individual crystal, was plotted using 100 particles. D_{90}, i.e., the length corresponding to 90% of the cumulative undersize particles, was determined from the size distribution plot. The effect of temperature on the CAM polymorphs was analyzed using a Leica LMV hot stage and Leica DMLP microscope. The samples were placed on clean glass slides and heated on hot stage at a heating rate of 20°C/min from 25 to 250°C and observed under optical and polarized modes.

Differential scanning calorimetry

Conventional differential scanning calometry (DSC) experiments were carried out using DSC Q2000 (TA instruments, Delaware, USA) equipped with a refrigerated cooling system and operating with Universal Analysis 2000 software version 4.5A. The instrument was calibrated for heat flow and temperature with high purity indium and zinc standards before analysis. The powder samples were accurately weighed, 3-5 mg, placed in T_{zero} aluminum pans and scanned using the DSC at a heating rate of 20°C/min from 25°C to 300°C under a nitrogen purge of 50 ml/min. All measurements were performed in triplicate.

Powder X-ray diffraction

Powder X- ray diffraction (PXRD) patterns of the samples were recorded at room temperature using Bruker's D8 Advance diffractometer (Karlsruhe, Germany) with CuKα radiation as a source (1.54) at 40 kV, 40 mA passing through a nickel filter and divergence slit (0.5°), antiscattering slit (0.5°) and receiving slit of 0.1 mm. The diffractometer was equipped with a 2θ compensating slit and was calibrated for accuracy of peak position and intensity with corundum. The diffractograms were collected in a continuous scan mode with a step size of 0.01° and step time of 1 second over an angular range of 3° to 40° 2θ. A powder sample (500 mg) was loaded into the sample holder made of poly methyl methacrylate (PMMA) and pressed by a clean glass slide to ensure co-planarity of the powder surface with the surface of the sample holder. The diffractograms were analyzed using Diffrac^{Plus} EVA software (v. 9.0).

Additionally, a variable temperature PXRD experiment was carried out for the amorphous forms of CAM and CAM-1. Powder samples were heated in the PXRD instrument from 25°C to 210°C and PXRD scans were collected at 10°C intervals.

Thermogravimetric analysis

Thermogravimetric analysis (TGA) was performed using a Mettler Toledo 851[e] TGA/SDTA (Mettler Toledo, Switzerland) and Star[e] software Solaris (v. 2.5.1). The samples, 5-7 mg, were weighed and analyzed under a nitrogen purge (50 ml/min) in aluminum crucibles at a heating rate of 20°C/min over a temperature range of 25-300°C. All measurements were performed in duplicate.

Generation of amorphous form

The *in situ* amorphous form of CAM was generated in DSC from CAM-2 through melting and cooling. The CAM-2 sample was heated from 25°C to 240°C at a heating rate of 20°C/min and held isothermally for 1 minute within the instrument. The molten sample was then cooled to 25°C at a rate of 20°C/min. The cooling rate of 20°C/min was sufficient to prevent the crystallization of CAM-2 to CAM-1, instead of yielding the amorphous form. High performance liquid chromatography (HPLC) analysis revealed that no degradation occurred during the process.

HPLC analysis

The *in situ* amorphous form of CAM was analyzed using an HPLC system (Shimadzu Corporation, Kyoto, Japan) comprising of a SCL-10A VP system controller, LC-10AT VP liquid chromatograph, FCV-10AL VP flow control valve, DGU-14A degasser, SIL-10AD VP auto-injector, CTO-10AS VP column oven, SPD-M20A prominence diode array (PDA) detector and a data acquisition Class-VP 6.10 software. The mobile phase was 0.035 mM of potassium dihydrogen orthophosphate (pH adjusted to 4.4) and Acetonitrile (70:30). All analyses were performed using Lichrospher® 100 RP-18e (5 µm) (Merck KGaA, Darmstadt, Germany) analytical column under isocratic condition at a flow rate of 1.0 ml/min at 25°C with 20 µl injection volume. The effluent was monitored at a wavelength of 210 nm. The method was validated for linearity, precision, accuracy and intra- and inter-day variability. Samples for the calibration curve generation were prepared in the mobile phase at a concentration range from 1 to 600 µg/ml. This stability indicating HPLC method, based on work previously carried out by Topalli *et. al.,* (18), was adopted to examine the degradation products of CAM. No degradation peaks for CAM were observed after the generation of the amorphous form. This was also confirmed using mass balance calculations.

Optimization of PXRD instrument parameters

Optimization of scan rate

The scan rate was optimized by assessing the effect of increment per step (step size) and step time individually based on the intensity and resolution of diffraction peaks of CAM-2. Step time was optimized by collecting PXRD patterns of 5% w/w CAM-2 in CAM-1 at varying step times (3, 4, 5, 6, 7, 9 and 11 seconds) and a constant step size of 0.05° 2θ. Step size was separately optimized by collecting diffractograms at various step sizes, 0.035°, 0.041°, 0.050°, 0.062°and 0.083° 2θ maintaining step time constant at 5 seconds.

Optimization of divergence and anti scatter slit width

PXRD patterns of 50% w/w CAM-2 in CAM-1 were collected at varying slit widths (0.1° to 0.8°). Optimization was carried out by assessing the effect of slit width on the intensity of peaks of CAM-2 and the closeness of experimental ratio of intensity of peaks of CAM-2 in a 1:1 mixture with CAM-1 and intensity of same peak in sample consisting of 100% CAM-2 with the calculated theoretical ratio.

Preparation of powder mixtures for analysis

Particle size of the analyte

Size reduction of the polymorphic forms was carried out using a pestle and mortar and an air

jet mill (Retsch Aeroplex, Spiral Jet Mill AS 50, Augsburg, Germany) with a grinding air pressure of 6 bars and a propellant air pressure of 1 bar. Maximum intensity was calculated in order to achieve the required theoretical optimum particle size.

Thickness of the powder bed

The thickness of the cavity of the sample holder was measured using a digimatic micrometer (Mitutoyo products, Japan). Minimum thickness of the powder bed required for quantification was calculated for the characteristic peaks of CAM-2 to ensure that the thickness of the sample packed into the holder is greater than the calculated minimum thickness required.

Optimization of sample preparation method

Commercial tablets of CAM were sourced from a local manufacturer and each tablet consisted of crystalline CAM (50.00%), starch (28.70%), microcrystalline cellulose (15.20%), sodium methyl paraben (0.10%), sodium propyl paraben (0.02%), croscarmellose sodium (1.00%), talcum (0.61%), magnesium stearate (0.68%), sodium starch glycolate (2.00%) and colloidal anhydrous silica (0.34%). Physical mixtures of 20% w/w and 50% w/w of CAM-2 in CAM-1 together with excipients similar to the aforementioned proportions were prepared in triplicate using the methods shown in Table 1.

Table 1 Methods used for sample preparation

SR. NO	SAMPLE PREPARATION METHOD	PROCEDURE
1	Geometric mixing of unmilled polymorphic forms with excipients (UM-GM)	Physical mixtures of unmilled CAM-1 and CAM-2 along with excipients were prepared by geometric mixing
2	Grinding in mortar and pestle followed by geometric mixing (PM-GM)	CAM-1 and CAM-2 were individually ground using a pestle and mortar, passed through a BSS sieve 150 followed by geometric mixing with the excipients
3	Grinding in air jet mill followed by geometric mixing (AJ-GM)	CAM-1 and CAM-2 were individually milled in an air jet mill, passed through a BSS sieve 150 followed by geometric mixing with the excipients
4	Grinding the premix of unmilled polymorphic forms with excipients using pestle and mortar (PREMIX-PM)	Physical mixtures of unmilled CAM-1 and CAM-2 were mixed with excipients followed by grinding and mixing using a pestle and mortar

The procedure for preparing the calibration curve stated here is valid only for the quantitative formula of the tablet investigated in this study. Nevertheless, the present study can provide a general framework for the quantification of polymorphs in solid dosage forms.

The diffractograms were analyzed with respect to the position and intensity of the peaks. The experimental ratio of (i) peak intensity of polymorphic forms (CAM-1 and CAM-2) that had been mixed with excipients and (ii) peak intensity of 100% CAM-2 that had been mixed with excipients was calculated. A co-relationship between the experimental ratio and theoretical calculated ratio was then established.

Preparation of calibration curve

Calibration curve for CAM-2

Physical mixtures of various weight fractions (80%, 84%, 88%, 92%, 96% and 100% w/w) of CAM-2 in CAM-1 together with excipients were prepared in triplicate using the optimized sample preparation method stated previously.

Calibration curve for CAM-1

Physical mixtures of various weight fractions (4%, 8%, 12%, 16%, 20% w/w of CAM-1 in CAM-2 together with the excipients, were prepared in triplicate using the optimized sample preparation method described previously.

Validation of analytical method and estimation of assay errors

The analytical method developed for the quantification was checked for linearity, accuracy and precision. In order to estimate assay errors, parameters such as instrument reproducibility, intra-day reproducibility, inter-day reproducibility, and the effect of packing of the sample were evaluated. Relative standard deviation (RSD) was then calculated.

The accuracy of the calibration curve was determined through examining independently concentrations of 82%, 90% and 94% w/w of CAM-2 in CAM-1 together with the excipients in triplicate and calculating the percentage recovery. Precision depicts the repeatability of measurements. Diffractograms were recorded for samples containing 82%, 90% and 94% w/w CAM-2 in CAM-1 multiple times and the RSD was calculated. Reproducibility of the instrument was assessed by recording diffractograms of 80% w/w CAM-2 in CAM-1 together with the excipients six times without removing the sample from the sample holder and the instrument. Intra-day reproducibility was estimated by acquiring diffractograms of 80% w/w CAM-2 in CAM-1 multiple times over a period of 8 hours. Inter-day reproducibility was estimated by recording diffractograms of 80 % w/w CAM-2 in CAM-1 along with excipients over a period of 5 days. The homogeneity of the sample mixing and the effect of variation due to crystal orientation was estimated by recording five times the diffractograms of refills of 80% w/w CAM-2 in CAM-1 together with the excipients.

Evaluation of commercial tablet formulation

Commercial tablets of CAM of 250 mg in strength were evaluated for the solid state of the API and weight fraction of the major form present. The tablet coating was removed using a surgical blade and the tablet core was then scraped to obtain a powder. The powder samples were subjected to PXRD analysis using the optimized step size (0.0625° 2θ), step time (9 seconds), divergence slit width (0.8°) and antiscatter slit width (0.8°). The analysis was performed in triplicate and % w/w of CAM-2 present in the tablets was determined.

RESULTS AND DISCUSSION

Solid state characterization

CAM-1 was found to exist as plate shaped crystals with a particle size ranging from 2.5 to 150 µm and D_{90} of 37 µm. The crystals exhibited pleochroic behavior when observed under a polarized light microscope. CAM-2 also showed plate shaped crystals with particle size ranging from 2 to145 µm and D_{90} of 26 µm exhibiting birefringence in polarized light. The images in optical and cross-polarized mode for CAM-1 and CAM-2 are shown in Figure 2. When the CAM-1 was subjected to hot stage microscopy, it exhibited a solid state transition to the CAM-2 at a temperature of about 150°C, evident by loss of pleochroic behavior which was further confirmed by DSC and PXRD studies and is discussed further below.

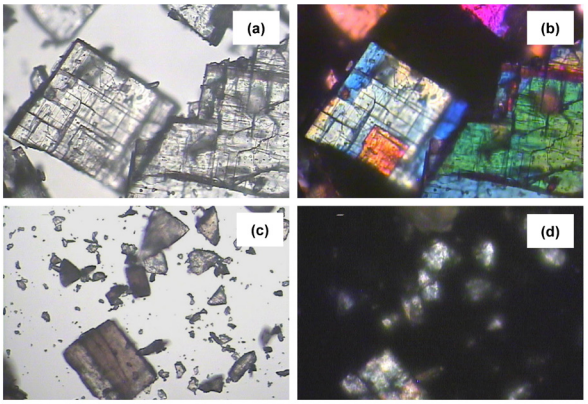

Figure 2 Microscopic images of CAM-1 in (a) optical and (b) polarized mode and CAM-2 in (c) optical and (d) polarized mode.

Figure 3 shows the DSC traces of CAM-2, CAM-1 and amorphous form of CAM. The DSC trace of CAM-1 showed an exothermic transition at about 151°C followed by a melting endotherm at 226.3°C. On the other hand, CAM-2 showed a sharp melting endotherm at 226.2°C. The amorphous form of CAM showed the onset of glass transition (T_g) at 106.0°C during heating followed by recrystallization at the range of 177.4°C to 209.0°C and melting at 216.5°C.

Optimization of PXRD instrument parameters

Instrumental parameters have been reported to affect the area of diffraction peaks (22). Therefore, instrumental parameters such as scan rate, divergence slit width and antiscatter slit width were optimized to obtain maximum

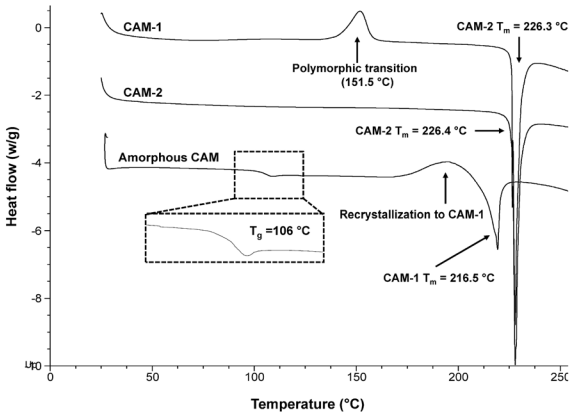

Figure 3 DSC traces of CAM-1, CAM-2 and amorphous CAM.

intensity and resolution of the peaks. This study was performed on pure CAM-2.

Optimization of scan rate

The intensity of peaks increased significantly as time increased up to 9 seconds. Figure 6 shows an increase in the intensity for a representative peak of CAM-1 with increasing step time. On the other hand, step size had no significant effect on the intensity of the peaks but, it affected the number of characteristic peaks of CAM-2. The number of peaks of CAM-2 were highest for a step size of 0.0625° 2θ. Figure 7 shows the effect of step size on the number of peaks of CAM-2. Thus, a step size of 0.0625° 2θ and step time of 9 seconds contributing to a scan rate 0.416° 2θ/min were selected as optimimum parameters and used for further analysis.

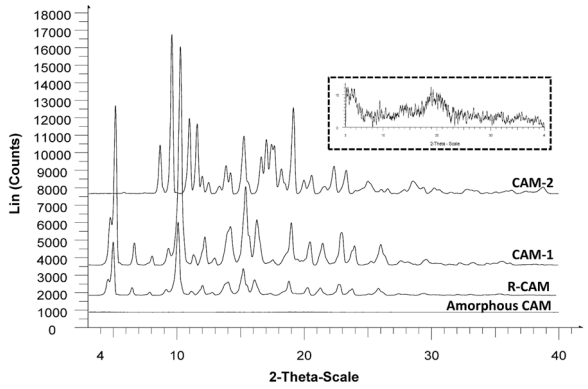

Figure 4 PXRD scans of amorphous CAM, amorphous CAM recrystallized to CAM-1 at 210 °C (R-CAM), CAM-1 and CAM-2. Inset shows enlarged version of PXRD scan of amorphous CAM.

Optimization of the divergence slit width and antiscatter slit width

The area of peaks characteristic to CAM-2 increased with an increase in the width of the divergence slit. The area of peaks was highest at a slit width of 0.8°. Additionally, the experimental intensity ratio (ratio of area of peaks for 50% w/w CAM-2 in CAM-1 and area of same peaks in pure CAM-2) approached close to the calculated ratio at a slit width of 0.8°. Therefore, the width for the divergence slit was selected as 0.8°. On the other hand, there was no significant change in the area of peaks with change in the width of antiscatter slit. It was used with a width of 0.8°.

Preparation of powder mixtures for analysis

Particle size of the analyte

Maximum particle size of the analyte required that optimum intensity could be calculated as proposed by Brindley (23) shown in Equation 1:

$$t_{max} = \frac{1}{100\,\mu} \qquad \text{Eq 1.}$$

where, t_{max} is the size and μ is the linear

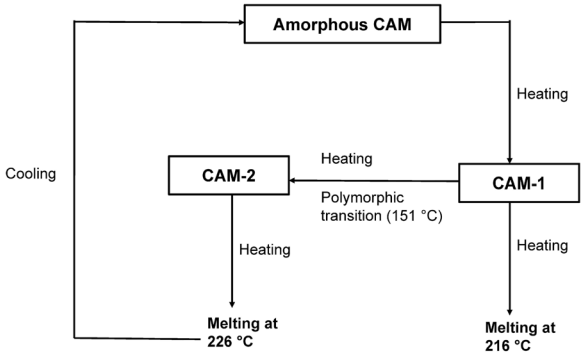

Figure 5 Schematic representation of temperature dependent conversions among CAM-1, CAM-2 and amorphous CAM.

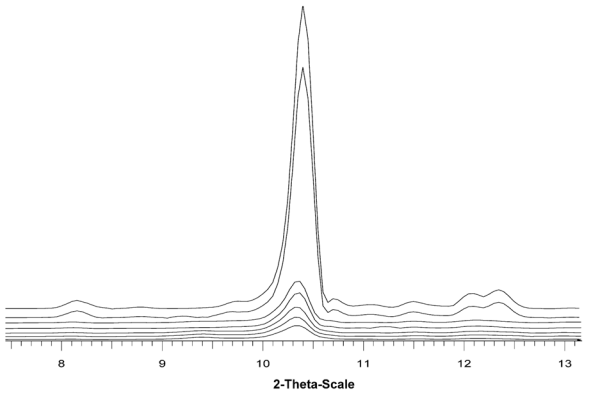

Figure 6 PXRD pattern showing an increase in intensity with increasing step time for a representative peak of CAM-1 at 10.4° 2θ. From bottom up, the diffractograms indicate step time of 3, 4, 5, 6, 7, 9 and 11 seconds, respectively, recorded at a constant step size of 0.05° 2θ.

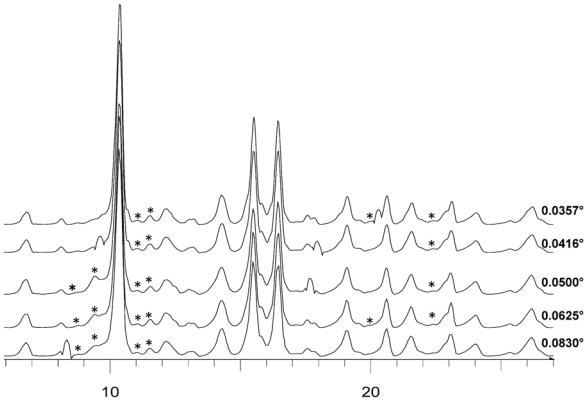

Figure 7 PXRD patterns of 5% w/w mixture of CAM-2 in CAM-1 at varying step size. Diffractograms were recorded at a constant step time of 5 seconds. "*" indicates identifiable peaks for CAM-2.

absorption coefficient of the analyte. μ is the summation of product of absorption coefficient and weight fraction of each individual element composing the analyte and can be calculated as shown in Equation 2:

$$\mu = \sum_1^n k\, W_k\, \mu_k \qquad \text{Eq. 2}$$

where, w is weight fraction of the element 'k' present 'n' number of times in the molecule of the analyte. μ for CAM was calculated using densities (ϱ_k) and the μ_k values of the elements at 0.008 Mev (energy corresponding to the wavelength of CuKα X-rays) were obtained from literature (24). Table 2 shows the calculated μ_k values for elements constituting CAM.

Table 2 Calculated μ_k values for elements in CAM

ELEMENT	W_k	μ_k/ρ_k (cm^2/g)	DENSITY	μ_k (cm^{-1})
Hydrogen	0.092	0.391	8.37×10^{-5}	0.3459×10^{-4}
Carbon	0.609	4.576	1.70	7.7792
Nitrogen	0.019	0.165×10^{-3}	1.16×10^{-3}	0.0088×10^{-1}
Oxygen	0.278	0.132×10^{-2}	1.33×10^{-3}	0.0155×10^{-2}

The μ value for CAM was determined as 4.88 cm^{-1} and the maximum particle size according to Equation 2 was determined as 20 μm. D_{90} of the milled CAM samples using air jet milling and pestle and mortar based trituration was 7.3 μm and 10.7 μm, respectively. Both methods generated samples with particle sizes below the limit of the maximum particle size (20 μm) that can be used for quantitative analysis.

The thickness of the powder bed in the sample holder

For maximum diffraction intensity from a flat powder specimen, the sample thickness must satisfy the conditions determined using Equation 3 (25):

$$t \geq \frac{3.2 \sin\theta}{\mu^* \rho} \qquad \text{Eq. 3}$$

Where, t is the thickness of the sample in the sample holder, μ^* is the mass absorption coefficient of the material of the powder and ϱ is the density of the powder including interstices calculated as the ratio of the weight of the sample taken and the volume of the sample holder.

The sample cell volume was determined as 0.49 cm^3 into which a 500 mg sample was packed. The ϱ value for the sample was 1.02 g/cm^3. The thickness of the cavity of the

sample holder (i.e., the thickness of the sample bed because the powder is packed so that the surface of the powder is coplanar with the surface of sample holder) was 1.006 mm. At the largest angle (22.3° 2θ), the minimum thickness of the powder bed was determined as 0.83 mm (see Equation 3), which was less than the experimental thickness of 1.006 mm. The thickness of the powder sample obtained during sample packing in the sample holder (1.006 mm) was greater than the ideal minimum values calculated for all the peaks.

Optimization of sample preparation method

The ratio of intensity of a peak of analyte in a sample consisting of certain weight fraction of analyte (I_i) and intensity of same peak in a sample consisting of 100% analyte (I_o) is provided by Equation 4 (26):

$$\frac{I_i}{I_0} = \frac{w_{\alpha 1}}{\left[w_{\alpha 1}\left(\mu_{\alpha 1} - \mu_{M1}\right) + \mu_{M1}\right]} x \frac{\left[w_{\alpha 1}\left(\mu_{\alpha 1} - \mu_{M2}\right) + \mu_{M2}\right]}{w_{\alpha 2}} \quad \text{Eq. 4}$$

where, 1 indicates the sample consisting of CAM-2, CAM-1 and excipients and 2 indicates the sample consisting of CAM-2 and excipients, w_α weight fraction of the analyte (CAM-2), μ_α and μ_M are the mass absorption coefficients for the analyte (CAM-2) and matrix, respectively. The meaning of the term 'matrix' is a composition without the analyte (CAM-2). Thus, μ_{M1} is the mass absorption coefficient for the matrix consisting of CAM-1 and excipients, while μ_{M2} is the mass absorption coefficient for the matrix consisting of only excipients.

The mass absorption coefficients of the excipients were calculated from the reported linear absorption coefficient values and the densities of each element present in the excipients. Table 3 shows the list of excipients together with their weight fractions and the calculated values of the mass absorption coefficients.

Table 3 Calculated mass absorption coefficient values for the excipients

EXCIPIENT	WEIGHT FRACTION	CALCULATED μ* (cm^2/g)
Starch NF	0.28	8.03
Microcrystalline cellulose NF	0.15	7.15
Croscarmellose sodium NF	0.01	11.75
Sodium starch glycolate NF	0.02	8.13
Magnesium stearate NF	0.006	6.30
Talc NF	0.006	35.82
Colloidal silicon dioxide NF	0.003	36.39
Sodium methyl paraben NF	0.001	9.73
Sodium propyl paraben NF	0.0002	8.93

PXRD patterns of the samples containing 20% w/w and 50% w/w CAM-2 in CAM-1 together with the excipients prepared by the four methods described previously were recorded using the optimized parameters. They were assessed for intensity ratios using the net area of the peaks. The mass absorption coefficient of matrix for 20% w/w CAM-2 and 50% w/w CAM-2 were determined as 6.5391 and 5.5347 cm^2/g, respectively. The value was determined as 3.9537 cm^2/g. Using Equation 4 the calculated intensity ratio values for the samples containing 20% w/w and 50% w/w CAM-2 in CAM-1 were 0.147 and 0.447, respectively.

The samples prepared using the PM-GM method showed a good correlation between the experimental and intensity ratios calculated ratios for peaks at a diffraction angle of 8.7° 2θ. The deviation of the experimental ratio from the calculated ratio for the samples prepared by other methods was attributed to shifts in the diffraction angles due to residual stress. A material experiences residual stress when it is subjected to mechanical or thermal processes. Size reduction of the polymorphic forms caused a shift in the diffraction angles. The shift was greatest in the samples prepared by air jet milling. The inter-planar spacing of a material that does not experience strain produces a characteristic diffraction pattern for that material. However, when it is strained, elongations or contractions are caused within the crystal lattice which changes the inter-planar

spacings of the lattice planes. This induced change in the d value results in a shift in the diffraction pattern (27). The magnitude of the shift was different for CAM-1 and CAM-2 which resulted in overlapping of peaks of both the polymorphic forms, thus making the characteristic peaks of both the forms indistinguishable.

The experimental intensity ratio of a peak at 8.7° 2θ correlated with the calculated values. The intensity increased proportionally to the concentrations for this peak. This occurred primarily because the peak of CAM-2 at 2θ 8.7° did not interfere with any of the peaks of CAM-1, due to the absence of peaks of CAM-1 close to 8.7°2θ. Additionally, amorphous halos in the excipients were observed in the 2θ range greater than 11°. The presence of amorphous halos of the excipients might have interfered with the intensity ratios for the peaks at diffraction angles greater than 2θ 11°. Figure 8 shows the PXRD patterns of the excipients used in the sample preparation and that of their physical mixture with CAM-1 and CAM-2.

Thus, a peak at 8.7° 2θ was selected for the quantification of CAM-2. The mixing method involving a particle size reduction of both the polymorphic forms, by separately grinding them in a mortar and pestle followed by mixing with the excipients (PM-GM), was used for further studies. This method resulted in the value of intensity ratios close to that of the calculated value.

Preparation of the calibration curve

The equation for intensity ratio (Equation 4) was modified to segregate the constants and variables to derive a modified Equation 5 as follows:

$$\frac{I_i}{I_0} = \frac{\left(\mu_1 - \mu_{M2}\right) + \frac{\mu_{M2}}{w_{\alpha 2}}}{\left(\mu_1 - \mu_{M1}\right) + \frac{\mu_{M1}}{w_{\alpha 1}}} \qquad \text{Eq. 5}$$

Equation 5 can be rewritten in the form of y = mx+c as follows:

$$\frac{I_i}{I_0} = \left(\mu_1 - \mu_{M2}\right) + \frac{\mu_{M2}}{w_{\alpha 2}} x \frac{1}{\left(\mu_1 - \mu_{M1}\right) + \frac{\mu_{M1}}{w_{\alpha 1}}} \qquad \text{Eq. 6}$$

Using the above equation, the calibration curve was plotted for CAM-2 shown in Figure 9a. Table 4 shows the values of μ_M and the values

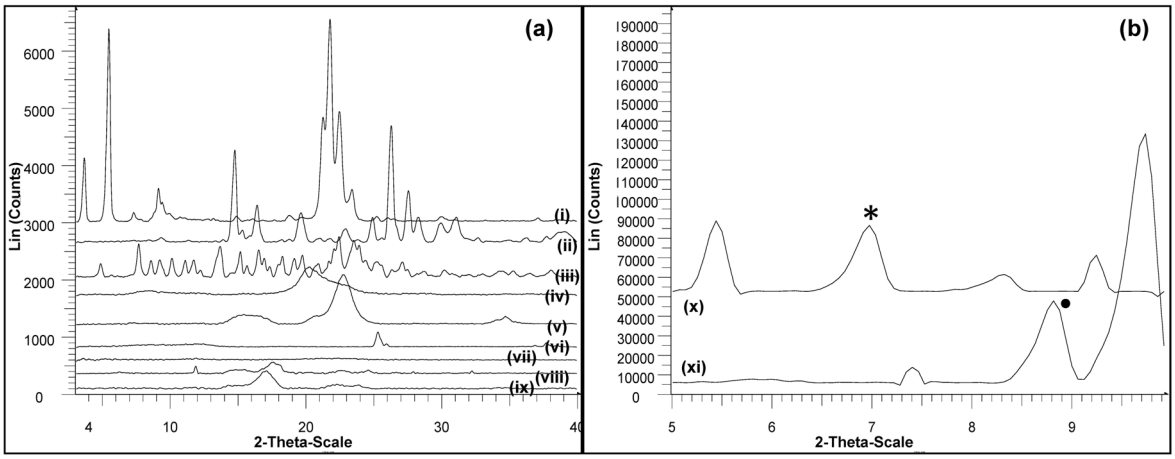

Figure 8 PXRD overlays of (a) Tablet excipients and (b) Physical mixture of CAM-1 with excipients and CAM-2 with excipients in 5 to 10° 2θ range. Key: (i) Magnesium stearate (ii) Sodium methyl paraben, (iii) Sodium propyl paraben, (iv) Crosscarmellose Sodium, (v) Microcrystalline cellulose, (vi) Talc, (vii) Aerosil 200, (viii) Sodium starch glycolate, (ix) Starch, (x) Physical mixture of CAM-1 with excipients and (xi) Physical mixture of CAM-2 with excipients. "*" and "●" represent characteristic peaks used for quantification of CAM-1 and CAM-2, respectively.

plotted on the X-axis for different proportions of CAM-2 and CAM-1.

Validation of the method and estimation of assay errors

The method developed here was linear with R^2 0.998 and accurate with recovery values in the range of 96.5 to 100.4%. It was precise with a percentage relative standard deviation (RSD) between 1.2-1.7%. Errors associated with PXRD such as, sample packing, intra- and inter-day variability may affect the assay.

Table 4 Calculated values of μ_M and term on X-axis for different weight fractions of CAM-2 and CAM-1

CAM-2			
% w/w CAM-2	μ_M		EXPERIMENTAL INTENSITY RATIO
80	4.59	0.078	0.714
84	4.46	0.082	0.769
88	4.33	0.087	0.837
92	4.20	0.091	0.881
96	4.08	0.096	0.949
100	3.95	0.1	1
CAM-1			
% w/w CAM-1	μ_M		EXPERIMENTAL INTENSITY RATIO
0	7.13	0	0
4	7.00	0.0029	0.039
8	7.87	0.0059	0.092
12	6.74	0.0091	0.140
16	6.62	0.0124	0.182

The RSD, due to sample repacking, was determined as 2.76% which showed good sample homogeneity after mixing and the absence of effect due to crystal orientation. The RSD due to inter-day and intra-day variability was determined as 1.50% and 0.67%, respectively. Tables 5 and 6 summarize the validation parameters and assay errors associated with the quantification of CAM-2.

Table 5 Validation parameters and assay error evaluation for 80-100% w/w calibration curve of CAM-2

PARAMETER	VALUE
R^2 of calibration curve	0.998
Recovery (%)	96.5-100.4
Precision (RSD)	1.2-1.7
Slope of the calibration curve	12.94
Intercept of the calibration curve	-0.294
Instrument reproducibility (RSD)	0.83
Intra-day variability (RSD)	0.67
Inter-day variability (RSD)	1.50
Sample packing (RSD)	2.76

Table 6 Accuracy and repeatability of the method for the quantification of CAM-2

ACTUAL	PREDICTED	% RECOVERY	RSD
82	81.7	99.6	1.41
90	88.7	98.6	1.20
94	93.0	98.9	1.70

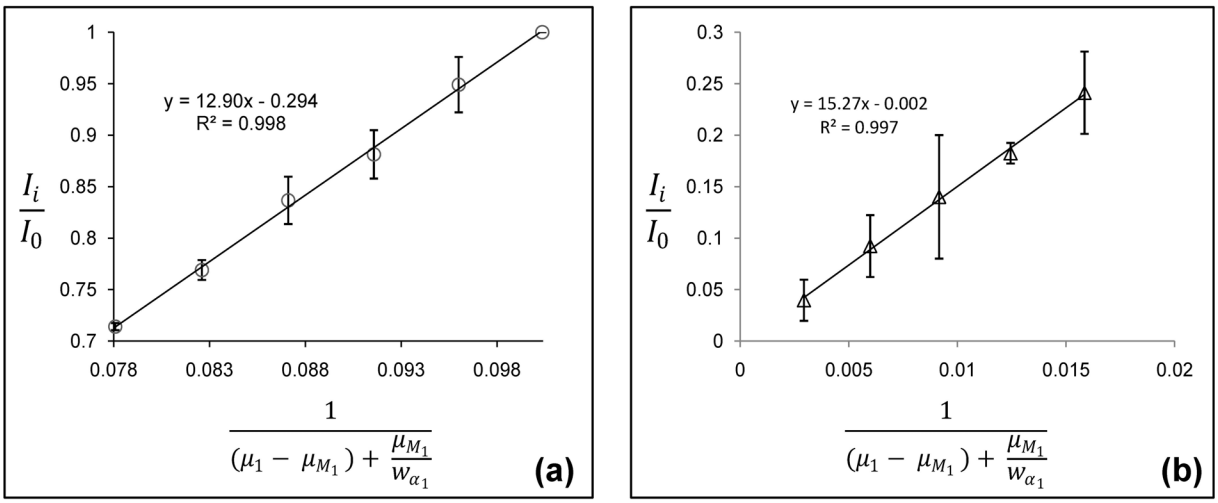

Figure 9 Calibration curve for (a) CAM-2 and (b) CAM-1.

Evaluation of the commercial formulation

PXRD analysis of the commercial tablet formulation showed the presence of CAM-2 as the major polymorph. The diffractogram showed the presence of all the characteristic peaks of CAM-2 and two characteristic peaks of CAM-1 at 5.2° and 6.7° 2θ, respectively. Figure 10 shows the PXRD pattern of the commercial formulation. The average intensity ratio of the peak at 8.7° 2θ was used to calculate the weight fraction of CAM-2 in the tablet. The average intensity ratio for CAM-2 was 0.978 and its weight fraction was calculated as 98% of the overall content of the API.

CAM-1 was present as a polymorphic impurity in the commercial tablet. The peaks of CAM-1 at 2θ value < 11° appeared in the diffractogram for the formulation. The characteristic peaks of CAM-1 at 2θ value >11° were not clear as these peaks either had merged with the peaks of CAM-2 or interfered with the amorphous halos of the excipients. In order to quantify CAM-1 in the tablet, its calibration curve was prepared in the concentration range of 0-20% w/w CAM-1 in CAM-2, together with excipients. A characteristic peak at 6.7° 2θ was used for analysis. The peak at 6.7° was also not affected by any peak of CAM-2 or by the amorphous halo of the excipients. The other characteristic peaks of CAM-1 were very close to the peaks of CAM-2 and the overlapping of few peaks was observed due to peak shift after the particle size reduction. The calibration curve for the quantification of CAM-1 in the commercial tablet is shown in Figure 9b. Table 4 shows the calculated values of μ_M, plotted on the x-axis and experimental intensity ratios obtained for various weight fractions of CAM-1. Tables 7 and 8 summarize the validation parameters and assay errors associated with the quantification of CAM-1. The limit of the the quantitation (LOQ) for CAM-1 was 4% w/w. The amount of CAM-1 present in the tablet formulation was approximately 2% w/w which was less than LOQ and could not be quantified.

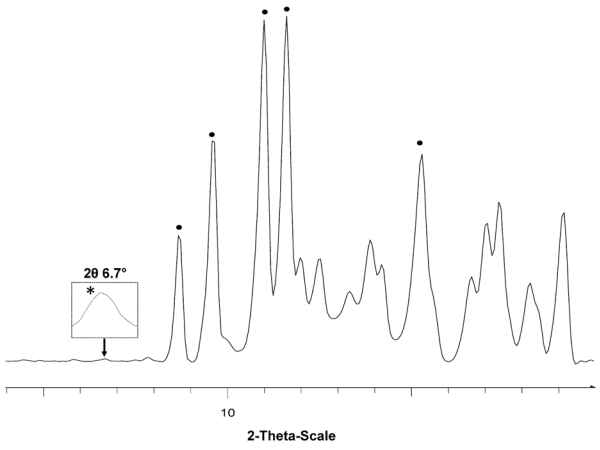

Figure 10 PXRD patterns of commercial tablet formulation. "*" and "●" represent characteristic peaks of CAM-1 and CAM-2, respectively.

CONCLUSION

In this study, clarithromycin was selected as a model drug for the evaluation of polymorphsin commercially available tablets. Differences in patterns of X-ray diffractograms were successfully utilized to quantify of polymorphs.

Table 7 Validation parameters and assay errors evaluation for 0-20% w/w calibration curve of CAM-1.

PARAMETER	VALUE
R^2 of calibration curve	0.997
Recovery (%)	96.6-107.0
Precision (RSD)	2.4-5
Slope of the calibration curve	15.27
Intercept of the calibration curve	-0.002
Instrument reproducibility (RSD)	0.0
Intra-day variability (RSD)	0.73
Inter-day variability (RSD)	2.26
Sample packing (RSD)	6.3

Table 8 Accuracy and repeatability of method for quantification of CAM-1

ACTUAL	PREDICTED	% RECOVERY	RSD
18	18.72	104.3	2.45
10	10.22	102.2	4.49
6	6.05	100.7	5.45

A PXRD based method for the quantification of clarithromycin Form I and Form II in the commercial tablet dosage form was developed. PXRD analysis revealed that the commercial tablet formulation contained Form II as the major polymorph and traces of Form I as a polymorphic impurity. This could have implications on the biopharmaceutical performance of clarithromycin when administered in tablet form.

REFERENCES

1 Agatonovic-Kustrin S, Rades T, Wu V, Saville D, Tucker IG. Determination of polymorphic forms of ranitidine-HCl by DRIFTS and XRPD. J Pharm Biomed Anal, 25(5-6): 741-750, 2001.

2 Tong HHY, Shekunov BY, Chan JP, Mok CKF, Hung HCM, Chow AHL. An improved thermoanalytical approach to quantifying trace levels of polymorphic impurity in drug powders. Int J Pharm, 295(1-2): 191-199, 2005.

3 Vippagunta SR, Brittain HG, Grant DJW. Crystalline solids. Adv Drug Deliv Rev, 48(1): 3-26, 2001.

4 Chawla G, Gupta P, Thilagavathi R, Chakraborti AK, Bansal AK. Characterization of solid-state forms of celecoxib. Eur J Pharm Sci, 20(3): 305-317, 2003.

5 Stephenson GA, Forbes RA, Reutzel-Edens SM. Characterization of the solid state: quantitative issues. Adv Drug Deliv Rev, 48(1): 67-90, 2001.

6 ICH Harmonised Tripartite Guideline. Specifications: Test procedures and acceptance criteria for new drug substance and new drug products: Chemical substances Q6A. Step 5 version. 65(251): 83041-63, 2000.

7 Zhang GGZ, Law D, Schmitt EA, Qiu Y. Phase transformation considerations during process development and manufacture of solid oral dosage forms. Adv Drug Deliv Rev, 56(3): 371-390, 2004.

8 Shah B, Kakumanu VK, Bansal AK. Analytical techniques for quantification of amorphous/crystalline phases in pharmaceutical solids. J Pharm Sci, 95(8): 1641-1665, 2006.

9 Alam S, Patel S, Bansal A. Effect of sample preparation method on quantification of polymorphs using PXRD. Pharm Dev Technol, 15(5): 452-459, 2010.

10 Suryanarayan R. Determination of relative amounts of the anhydrous carbamazepine in a mixture by powder x-ray diffarctometry. Pharm Res, 6(12): 1017-1024, 1989.

11 Tiwari M, Chawla G, Bansal AK. Quantification of olanzapine polymorphs using powder X-ray diffraction technique. J Pharm Biomed Anal, 43(3): 865-872, 2007.

12 Patel S, Kaushal AM, Bansal AK. Compression physics in the formulation development of tablets. Crit Rev Ther Drug, 23(1): 23(1): 1-65, 2006.

13 Suryanarayanan R, Herman CS. Quantitative analysis of the active ingredient in a multi-component tablet formulation by powder X-ray diffractometry. Int J Pharm, 77(2-3): 287-295, 1991.

14 Suryanarayanan R, Herman CS. Quantitative analysis of the active tablet ingredient by powder X-ray diffractometry. Pharm Res, 8(3): 393-399, 1991.

15 Noguchi S, Fujiki S, Iwao Y, Miura K, Itai S. Clarithromycin monohydrate: a synchroton X-ray powder study. Acta crystallogr E, 68(3): 667-668, 2012.

16 Noguchi S, Miura K, Fujiki S, Iwao Y, Itai S. Clarithromycin form I determined by synchrotron X-ray powder diffraction. Acta Crystallogr C, 68(2): 41-44, 2012.

17 Tian J, Thallapally PK, Dalgarno SJ, Atwood JL. Free transport of water and CO_2 in nonporous Hydrophobic clarithromycin form II crystals. J Am Chem Soc, 131(37): 13216-13217, 2009.

18 Topalli S, Rao BN, Annapurna M, Sharma A, Chandrashekhar TG. Development and validation of high performance liquid chromatography method for quantification of related substances in clarithromycin powder for an oral suspension dosage form. Int J Anal Pharm Biomed Sci, ISSN:2278-0246, 1-12, 2012.

19 Van Santen RA. Comment on "entropy production and the Ostwald step rule". J Phys Chem, 92(1): 248, 1988.

20 Tozuka Y, Ito A, Seki H, Oguchi T, Ymamoto K. Characterization and quantitation of clarithromycin polymorphs by powder X-ray diffractometry and solid-state NMR spectroscopy. Chem Pharm Bull, 50(8): 1128-1130, 2002.

21 Burger A, Ramberger R. On the polymorphism of pharmaceuticals and other molecular crystals. Microchim Acta, 72(3-4): 259-271, 1979.

22 Hurst VJ, Schroeder PA, Styron RW. Accurate quantification of quartz and other phases by powder X-ray diffractometry. Anal Chim Acta, 337(3): 233-252, 1997.

23 Brindley, GW. The X-ray identification and crystal structures of clay minerals, in Brown, G (ed), The X-ray identification and crystal structures of clay minerals. *Mineralogical society*, London, pp 492, 1961.

24 Hubbell JH, Seltzer SM. X ray mass attenuation coefficients. http://www.nist.gov/pml/data/xraycoef/index.cfm. Accessed 9 September 2012.

25 Garner, WE. Chemistry of the solid state. *Academic press*, New York, 1955.

26 Brittain, HG. Physical characterization of pharmaceutical solids. *Marcel Dekker*, New York, pp. 199-208, 1995.

27 Xu LH, Jiang DD, Zheng XJ. Effect of grain orientation in x-ray diffraction pattern on residual stress in polycrystalline ferroelectric thin film. J Appl Phys, 112(4): 43521, 2012.